Modeling of Double Excitation Synchronous Motors Using Nodal Based – Generalized Equivalent Magnetic Circuit

Trung-Kien Hoang, K Hoang, L Vido, F Gillon, M. Gabsi

ISEF 2015 - XVII International Symposium on Electromagnetic Fields
in Mechatronics, Electrical and Electronic Engineering

Valencia, Spain, September 10-12, 2015

Modeling of Double Excitation Synchronous Motors Using Nodal Based – Generalized Equivalent Magnetic Circuit

K. Hoang[1] , L. Vido[2], F. Gillon[3] , and M. Gabsi[1]

[1]SATIE, ENS Cachan, 94230 Cachan, France

[2]SATIE, Université de Cergy – Pontoise, 95000, France

[3]LE2P, Ecole Centrale de Lille, 59650 Villeneuve d'Ascq Cedex, France

Abstract – ***The utilization of nodal based – generalized equivalent magnetic circuit method (EMCM) in the modeling of a double excitation synchronous machine (DESM) is presented in this paper. Nonlinear magnetization characteristic is taken into consideration. This method shows a distinguishing advantage over the finite element method (FEM) in term of computation time. The validity of the EMC results are examined by comparisons with 3D FEM.***

I Introduction

A Double Excitation Synchronous Motor (DESM) proposes additional windings in a Permanent Magnet Synchronous Motor (PMSM) [1]. Such kind of structure combines advantages of PMSMs with high power density and high efficiency and ones from wound field synchronous motor with capability of regulating flux in the air-gap. Several papers have been presented focusing on DESM [1- 4].

In the motor design phase, an enormous number of evaluations are usually iteratively taken, for example an optimization process. Therefore a model with acceptable accuracy but fast to evaluate is obviously prioritized to mitigate the burden on computation time. Finite element method (FEM) is traditionally chosen as a high fidelity model; however, the inherent disadvantage of this method is time consuming especially with three dimensional modeling. In contrast to FEM, equivalent magnetic circuit method (EMCM) provides a noticeable compromise between computation time and accuracy. This method with a concept of flux tube transforms the motor into a magnetic circuit presented by nodes, reluctance and magneto-motive force (MMF).

This paper aims to presents the EMC method in 3D configuration to handle the modeling of a DESM. The EMCM discussed in this paper is based on nodal formulation i.e. the Kirchhoff's voltage law is used to establish the equations system [5]. Also, the model will be divided into a mesh of reluctances characterized by number of columns and rows (generalization), the sizes of elements are flexibly controlled. By doing this, it is able to explore local information of the motor. The validity of the analysis results are verified by comparisons with 3D FEM ones.

ISBN: 978-84-606-9102-0

II Double Excitation Synchronous Motor

A number of motor prototypes using double principle have been realized with regard to different criteria. Concerning the localization of the excitation flux sources, both sources could be placed in the stator, rotor or mixed. According to the type of flux combination, a DESM could be classified as series or parallel. Fig. 1 shows the reference model of DESM used in this paper [3].

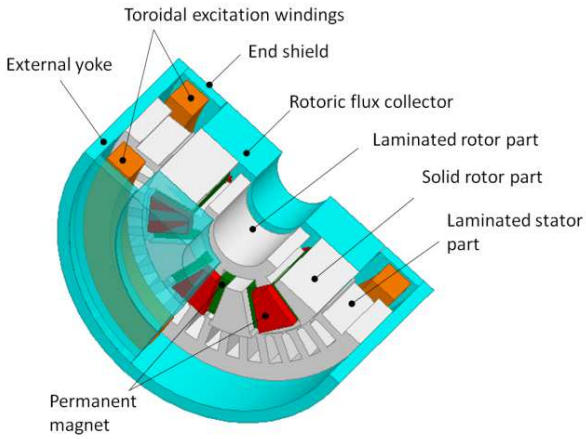

Fig. 1 Studied DESM model

This reference belongs to parallel type which is proved to be advantageous over a series configuration with respect to controlling open circuit flux [6]. The main reason deciding on this parallel type is due to the main flux path generated by field winding does not pass through permanent magnets (PMs) that helps the model avert from demagnetization. In this prototype, two toroidal field windings are placed on the stator side; therefore, sliding contacts are avoided. Ferrite PMs are located in the rotor using flux concentration principle to increase air-gap flux. Details of the studied model are given in Table 1. One should be noted that, in this prototype, the motor flux lines are truly three dimensional as in [3], so that solid core material are advised in some regions of the motor marked in Fig. 1.

TABLE 1: CONFIGURATION OF STUDIED MODEL

Parameters	Value
Number of phases	3
Number of turns per phase	33
Number of turns per DC winding	150
Number of poles	12
Motor length	115 mm
Outer stator diameter	92 mm
Inner stator diameter	57.5 mm
Number of slots	36
Air-gap length	0.5 mm
PM residual flux density	0.4 T (ferrite PM)
Based speed	2000 rpm
Rated power	3 kW

III Generalized EMCM with DESM model

EMCM has long been proven as an effective alternative tool for motor analysis with a much shorter computation time while maintaining close results compared to FEM [7 - 11]. Using EMCM is also advantageous over FEM when there is a need to couple with other analyses such as thermal or acoustic ones [12]. In EMCM, two important circuit laws guiding equation system formulation namely Kirchhoff's current and Kirchhoff's voltage laws. These lead to nodal based and mesh based equations, respectively [5]. This paper employs Kirchhoff's current law which is the most common method due to the ease of establishing and extending equation system compared to the latter one.

Regarding the reluctance mesh formulation, two alternatives are proposed: lumped parameter model as in [13, 10, 14] and generalized model [15 - 17]. Basically, a lumped parameter model requires a prior knowledge of critical flux paths of the machine. A small number of reluctances are presented based on main pre-assumed flux paths. On the contrary, by mean of generalization as will be demonstrated in this paper, each part of the motor is divided into a mesh of elements characterized by a number of rows and columns. The reluctance network establishment will be detailed in this section.

Electromagnetic concept of EMCM

Conventionally, two methods could be used with EMCM are tooth contour [18] and flux tubes [19]. In this research, flux tubes method which is the most popular implementation of EMCM will be employed. The flux is considered to be constant inside the tube. A basic expression for reluctance and permeance calculations of the flux tube are given by (1) and (2) respectively.

$$R = \int_0^L \frac{dl}{\mu_0 \mu_r S(l)} \tag{1}$$

$$P = \frac{1}{R} \tag{2}$$

where L is length of the tube , S is cross section of the tube at position l. μ_r is the relative permeability of the tube material and μ_0 is the permeability of the air.

A permanent magnet can be modeled by a reluctance connected in series with an equivalent MMF as (3):

$$M_{pm} = \frac{B_r h_m}{\mu_0 \mu_r} \tag{3}$$

where h_m and B_r are magnet thickness and residual magnetic flux density respectively.

Phase MMFs are put in the stator teeth with net value is given by (4):

$$M_{phase} = N_t (i_1 - i_2) \tag{4}$$

Where N_t is number of phase turns, i_1 and i_2 are phase currents flowing in the winding accommodated in the slot. (4) is based on an assumption that i_1 and i_2 are axially going in the same direction.

Network formulation for DESM

With the generalized EMCM, flux paths are limited to only tangential and radial directions making the basic bi-directional element consists of 4 reluctances in 2 directions as shown in Fig. 2.

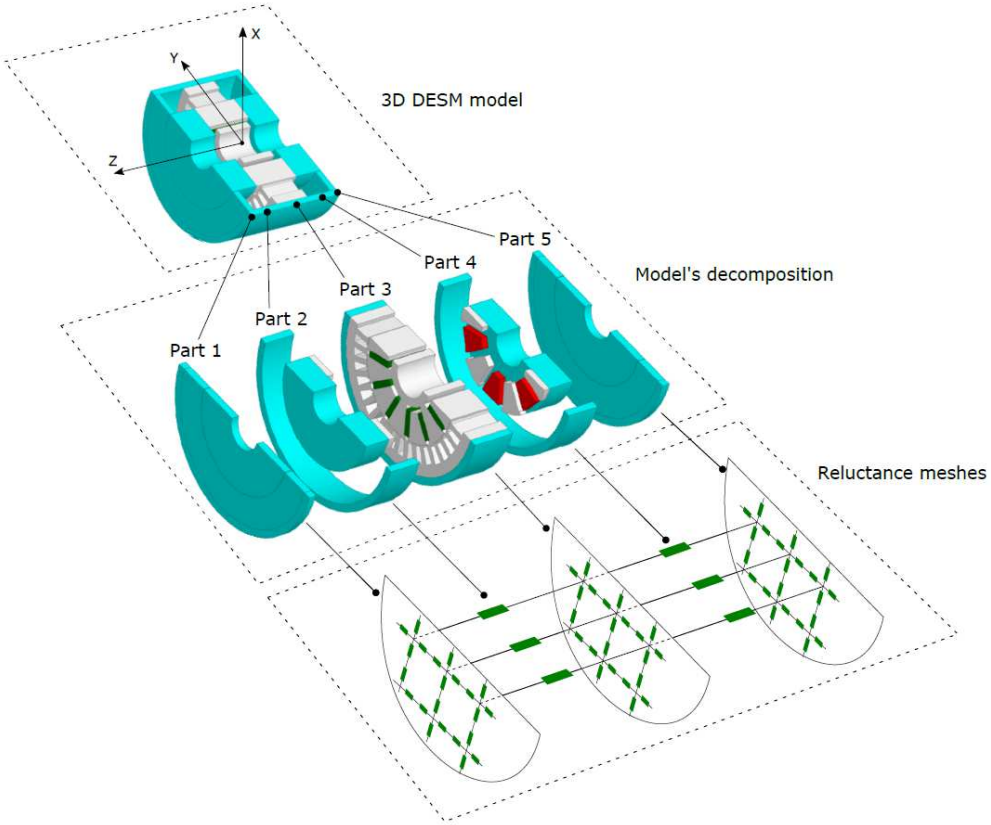

a) Motor disassembling for reluctance network

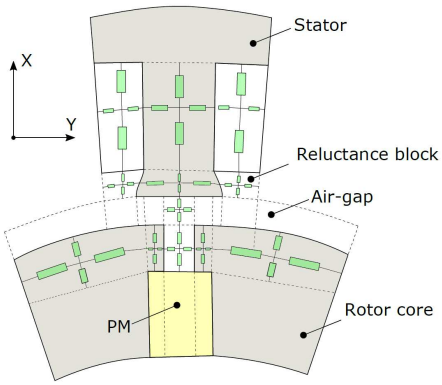

b) Typical reluctance mesh for part 3

Fig. 2 Generalized reluctance mesh

Flux paths of the prototype analyzed in this work are truly 3D; therefore, additional reluctances in the axial direction must be provided. To handle this formulation, the model is disassembled into 5 parts as shown in Fig. 2a, in which parts 1 and 5 are almost identical (symmetric over the X-Y plane), this similar symmetry is applied the same for parts 2 and 4. In order to be less complicated, reluctance network formulation is based on an assumption that flux in parts 1, 3 and 5 are 2D (in X and Y directions). Whereas flux in parts 2 and 4 are assumed in axial direction (Z). In other word, parts 2 and 4 function as a flux bridge to connect part 3 with the pair parts 1 and 5; therefore parts 2 and 4 will be represented by a number of uni-directional reluctances. This assumption is acceptable due to the fact that flux in part 1, 2, 4 and 5 are almost solely DC flux from side PMs (PMs in red) and DC field windings.

The mesh in part 3 is more complicated due to a complex and different geometries appeared as in Fig. 2b for a visualization purpose. Stator and rotor part contains a number of layers (columns),

each layer is a row of bi-directional elements. Regarding the detail property of regions, 1 layer is dedicated to the stator tooth tip. In all other paths (for example tooth parts, yoke, PMs etc.), number of layers is flexible controlled to ensure a general guide such that being closer to the air-gap, the mesh should be denser. Mesh generation must match element boundaries with material boundaries (cores, PMs and air). The mesh building principle for parts 1 and 5 are quite the same as one of part 3 except they are much simpler.

The air-gap mesh is rather different compared to stator and rotor meshes. It is still based on bi-directional element, however, the creation is derived from stator and rotor meshes in a manner that: every edge of elements of stator and rotor (contiguous with the air-gap) define edges of air-gap's elements as shown in Fig. 2b. Air-gap mesh will be redefined for a new rotor position i.e. taking into account motor's rotation.

With the aim to reduce computation time, the analysis will be performed for only one pole pair. To this end, the periodic condition is applied by simply connecting the nodes at first angular position with ones corresponding to one pole pair (60 mechanical degree in this case).

After mesh creation process is finished, the nodal magnetic potentials are obtained by solving (5):

$$\begin{bmatrix} P_{11} & P_{12} & \dots & P_{1N} \\ .. & & & \\ P_{N1} & P_{N2} & \dots & P_{NN} \end{bmatrix} \begin{bmatrix} U_1 \\ .. \\ U_N \end{bmatrix} = \begin{bmatrix} \phi_1 \\ .. \\ \phi_N \end{bmatrix} \tag{5}$$

Where N is number of nodes, is the sum of flux source connected to node "*i*", U_i is the magnetic potential of node "*i*" and [*P*] is the permeance matrix defined by (6)

$$P_{ij} = \begin{cases} -p_{ij} & \text{if } i \neq j \\ \sum_{k=1,k\neq i}^{N} p_{ik} & \text{if } i = j \end{cases} \tag{6}$$

with $p_{i,j}$ is permeance connection between node "*i*" and node "*j*".

Based on solved magnetic potentials, non-linear property could be achieved by iteratively updating permeabilities based on B-H magnetization curve. Algorithm block diagram is illustrated in Fig. 3

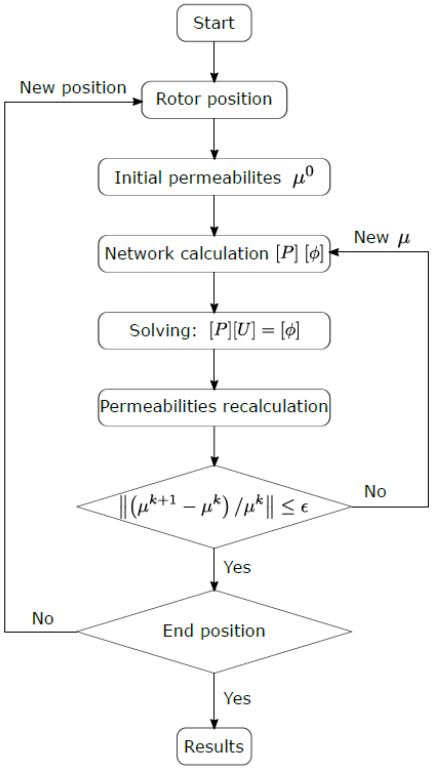

Fig. 3 Algorithm diagram for non-linearity solving

IV Results and verification with FEM

In order to verify the EMCM results (implemented by MATLAB), comparisons with 3D FEM are conducted. The tangential and radial components of air-gap flux density distribution for one pole pair at aligned position, no-load and field windings are not excited are displayed in Fig. 4.

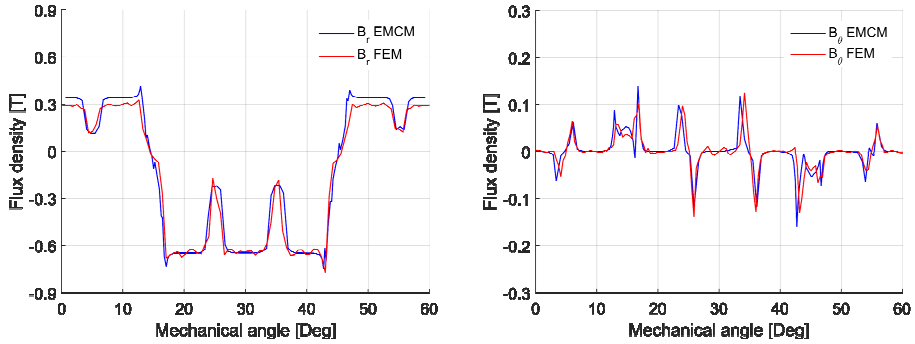

a) Radial component b) Tangential component

Fig. 4 Air-gap flux density distribution (@ no-load, un-excited, aligned position)

A good comparison agreement is seen for radial air-gap flux density; however, bigger difference is seen with tangential components, this could be explained as tangential flux density is very prone to the mesh around air-gap region. The FEM analysis for DESM in this research is 3D so that a very fine mesh is especially constrained by computer's memory. For this air-gap flux density calculation, the FEM analysis uses around 161000 elements while the number of elements for EMCM is 1100 i.e. 150 times less. As observed in Fig. 4a, the radial flux density is asymmetric between first half and second half of one pole pair. This happens owing to the homopolar topology of the studied DESM [3] in which when field currents are set to zero, air-gap flux densities in the concentrated area are reported to be higher than other one.

Electromagnetic torque is calculated based on virtual work principle which uses energy variation stored in the area closed by the flux and MMF [20, 21] given by (7). This method utilizes phase fluxes and currents which are global quantities instead of local one (used in Maxwell stress tensor method) that usually requires a denser mesh and hence a longer computation time.

$$T = mp\frac{\Delta W}{2\pi} \tag{7}$$

where m is the number of phases, p is the number of pole pairs and ΔW is the co-energy converted per phase over an electrical period.

Torque generation at zero load angle and different load conditions (full-load at phase current of 10 A) are displayed in Fig. 5a.

As aforementioned, a distinguishing feature of DESM is flux control capability either reducing or enhancing air-gap flux. The flux is; therefore, varies according to changes in field currents. Fig. 5b represents maximum flux per phase per turn as function of field current. It should be noted that due to thermal limit, maximum field current of 6 A is applied. For computations in Fig. 5, element numbers for FEM and EMCM are about 58000 and 530 respectively. The one point computation time for FEM and EMCM are 72 s and 0.16 s. A good accordance can be seen in the comparisons confirm the accuracy of the proposed EMCM.

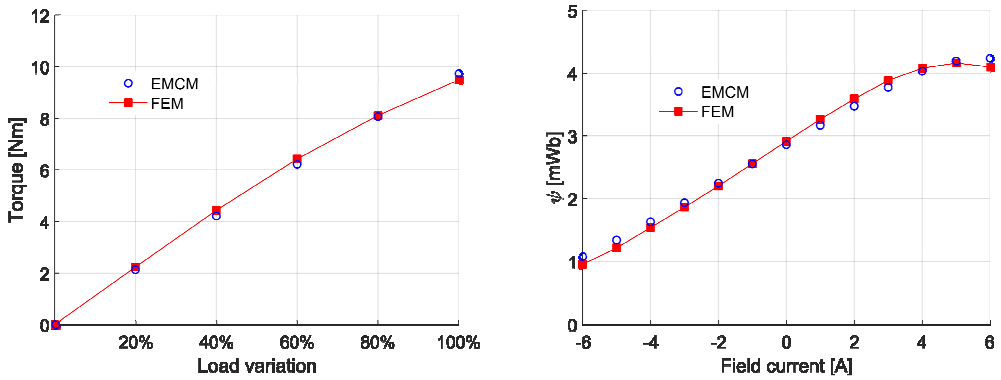

a) Torque according to load variation b) Maximum flux according to field current

Fig. 5 Torque and flux comparisons according to load variation

V Conclusion

A generalized EMCM has been applied to 3D configuration of a DESM with the algorithm to solve nodal magnetic potentials. The proposed method takes into account the nonlinear behavior of the materials and also the rotor rotation. The EMCM is proved to be useful with accurate results while keeping a much shorter computation time compared to FEM analysis. This promises a good application in the design stage of the motor, for example, an optimization process.

VI References

[1] Y. Amara, L. Vido, M. Gabsi, E. Hoang, A. Hamid Ben Ahmed, and M. Lecrivain, "Hybrid excitation synchronous machines: Energy-efficient solution for vehicles propulsion," *Vehicular Technology, IEEE Transactions on*, vol. 58, no. 5, pp. 2137–2149, Jun 2009.

[2] D. Fodorean, A. Djerdir, l.-A. Viorel, and A. Miraoui, "A double excited synchronous machine for direct drive application: Design and prototype tests," *Energy Conversion, IEEE Transactions on*, vol. 22, no. 3, pp. 656–665, Sept 2007.

[3] V. Lionel, G. M, L. M, and A. Y, "Homopolar and bipolar hybrid excitation synchronous machines." Proc. IEEE Int. Electric Machines and Drives Conf IEMDC, May 2005, pp. 1212–1218.

[4] B. Nedjar, S. Hlioui, Y. Amara, L. Vido, M. Gabsi, and M. Lecrivain, "A new parallel double excitation synchronous machine," *Magnetics, IEEE Transactions on*, vol. 47, no. 9, pp. 2252–2260, Sept 2011.

[5] H. Derbas, J. Williams, A. Koenig, and S. Pekarek, "A comparison of nodal- and mesh-based magnetic equivalent circuit models," *Energy Conversion, IEEE Transactions on*, vol. 24, no. 2, pp. 388–396, June 2009.

[6] Y. Amara, S. Hlioui, R. Belfkira, G. Barakat, and M. Gabsi, "Comparison of open circuit flux control capability of a series double excitation machine and a parallel double excitation machine," *Vehicular Technology, IEEE Transactions on*, vol. 60, no. 9, pp. 4194–4207, Nov 2011.

[7] B. Bekkouche, A. Chaouch, and Y. Mezari, "A switched reluctance motors analyse using permeance network method," *International Journal of Applied Engineering Research*, vol. 1, no. 2, pp. 137–152, 2006.

[8] K. Tajima, K. Sato, T. Komukai, and O. Ichinokura, "Reluctance network analysis of an orthogonal-core type parametric induction motor," *Magnetics, IEEE Transactions on*, vol. 35, no. 5, pp. 3706–3708, Sep 1999.

[9] K. Nakamura and O. Ichinokura, "Dynamic simulation of pm motor drive system based on reluctance network analysis," in *Power Electronics and Motion Control Conference, 2008. EPE-PEMC 2008. 13th*, Sept 2008, pp. 758–762.

[10] K. Chau, M. Cheng, and C. Chan, "Nonlinear magnetic circuit analysis for a novel stator doubly fed doubly salient machine," *Magnetics, IEEE Transactions on*, vol. 38, no. 5, pp. 2382–2384, Sep 2002.

[11] H. Polinder, J. Slootweg, M. Hoeijmakers, and J. Compter, "Modeling of a linear pm machine including magnetic saturation and end effects: maximum force-to-current ratio," *Industry Applications, IEEE Transactions on*, vol. 39, no. 6, pp. 1681–1688, Nov 2003.

[12] N. Bracikowski, M. Hecquet, P. Brochet, and S. Shirinskii, "Multiphysics modeling of a permanent magnet synchronous machine by using lumped models," *Industrial Electronics, IEEE Transactions on*, vol. 59, no. 6, pp. 2426–2437, June 2012.

[13] Z. Zhu, Y. Pang, D. Howe, S. Iwasaki, R. Deodhar, and A. Pride, "Analysis of electromagnetic performance of flux-switching permanent-magnet machines by nonlinear adaptive lumped parameter magnetic circuit model," *Magnetics, IEEE Transactions on*, vol. 41, no. 11, pp. 4277–4287, Nov 2005.

[14] M. Bash, J. Williams, and S. Pekarek, "Incorporating motion in mesh-based magnetic equivalent circuits," *Energy Conversion, IEEE Transactions on*, vol. 25, no. 2, pp. 329–338, June 2010.

[15] M. Amrhein and P. Krein, "Magnetic equivalent circuit modeling of induction machines design-oriented approach with extension to 3-d," in *Electric Machines Drives Conference, 2007. IEMDC '07. IEEE International*, vol. 2, May 2007, pp. 1557–1563.

[16] J. Perho, "Reluctance nework for analysing induction machines," Ph.D. dissertation, Helsinki University of Technology, 2002.

[17] D. Gomez, A. Rodriguez, I. Villar, A. Lopez-de Heredia, I. Etxeberria-Otadui, and Z. Zhu, "Improved permeance network model for embedded magnet synchronous machines," in *Electrical Machines (ICEM), 2014 International Conference on*, Sept 2014, pp. 1231–1237.

[18] E. Ilhan, J. Paulides, L. Encica, and E. Lomonova, "Tooth contour method implementation for the flux-switching pm machines," in *Electrical Machines (ICEM), 2010 XIX International Conference on*, Sept 2010, pp. 1–6.

[19] V. Ostovic, *Dynamics of saturated machines*. Springer-Verlag, 1989.

[20] D. Staton, W. Soong, and T. Miller, "Unified theory of torque production in switched reluctance and synchronous reluctance motors," *Industry Applications, IEEE Transactions on*, vol. 31, no. 2, pp. 329–337, Mar 1995.

[21] C. Cossar, M. Popescu, T. Miller, M. McGilp, and M. Olaru, "A general magnetic-energy-based torque estimator: Validation via a permanent-magnet motor drive," *Industry Applications, IEEE Transactions on*, vol. 44, no. 4, pp. 1210–1217, July 2008.